Electronic Supplementary Material (ESI) for Journal of Materials Chemistry B.

Supporting Information

Hydroxyapatite Nanowhiskers Embedded in Chondroitin Sulfate Microspheres as Colon Targeted Drug Delivery System

Thelma Sley P. Cellet, Guilherme M. Pereira, Edvani C. Muniz, Rafael Silva and Adley F. Rubira*

Departamento de Química, Universidade Estadual de Maringá, Avenida Colombo 5790, CEP: 87020-900 - Maringá, Paraná, Brazil.

1. Additional Features on FTIR of Hydroxyapatite Nanowhiskers

In addition to the discussed in the manuscript for the FTIR spectrum, Figure 1, some additional features are observed and interpreted. The intense bands at 1049 cm^{-1} and 1095 cm^{-1} are vibration mode ν_3 of phosphate groups. The band at 962 cm^{-1} is the ν_1 mode. The bands of phosphate groups with ν_4 mode are observed at 633, 602 and 566 cm^{-1}. The splitting of ν_4 mode in three peaks indicates the low site symmetry of phosphate specie in the crystal lattice, and confirms its presence in different lattice positions for the distinction. It is also observed ν_2 mode at 470 cm^{-1}.

In relation to the presence of carbonate species in the hydroxyapatite particles, it is possible to observe the band at 876 cm^{-1} that is due to carbonate ν_2 vibration mode. The band related to the carbonate vibration mode ν_1 not appear in the spectrum, since it occurs in the same region of the ν_3 vibration band of phosphate groups, which in this case is a much more intense band.

2. Synthesis CS-methacrylate

Chondroitin sulfate (CS) is a water soluble polymer, so its use in the preparation of microparticles for drug is done by is modification with the addition of a pendent group to promote the formation of cross-links, which results in a cross-linked glycosaminoglycan. The approach used is the modification of CS with glycidyl methacrylate (GMA), to generate methacrylate pendent groups in the CS chains. Reaction mechanisms between CS and GMA have been reported [1, 2]. It is based on the reaction of the epoxy group of GMA with carbonyl group of CS. Different physical properties can be obtained after crosslinking the chains depending on the degree of methacrylation. In the present work, CS methacrylation was carried out in aqueous acid medium. It is a slow and irreversible reaction and it can generate two

different products depending on the position in which the epoxide group of GMA reacts, the 3-methacryloyl-2-glyceryl ester or the 3-methacryloyl-1-glycerol ester. The reaction scheme is presented in the Figure S1. This is due to the ability of hydroxyl groups attacked GMA at different positions of the epoxide ring.

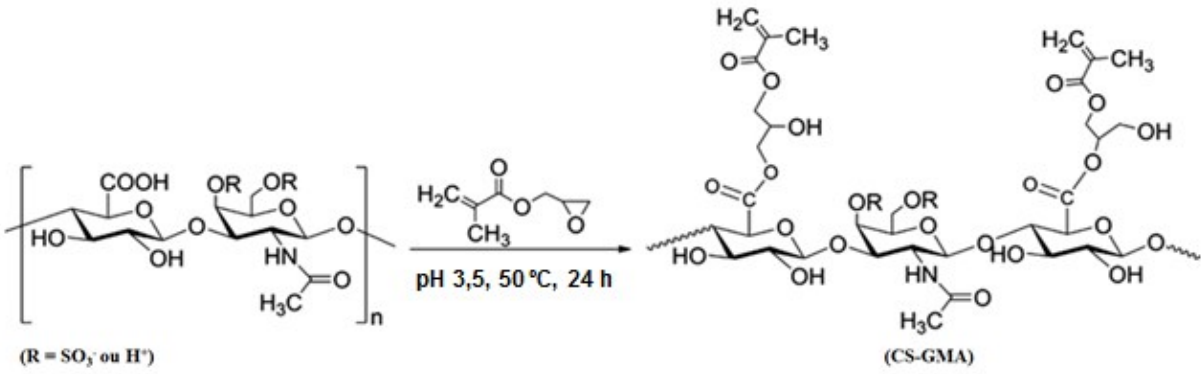

Figure S1. Reaction of CS with GMA in acid aqueous medium.

Chemical modification of the CS with GMA was analyzed by FTIR. In the Figure S2 are shown FTIR spectra of pure GMA, pristine CS and CS-methacrylate. The spectrum of the CS-methacrylate, Figure 6 (c) shows all characteristic bands of CS and the modification is evidenced by the appearance of the band at 1746 cm^{-1}, related to the stretching of the carbonyl groups (ν C=O) of esters and due to an increase in the intensity of band at 1642 cm^{-1}, related to carbon-carbon double bonds (ν C=C) of the conjugated system [3] .

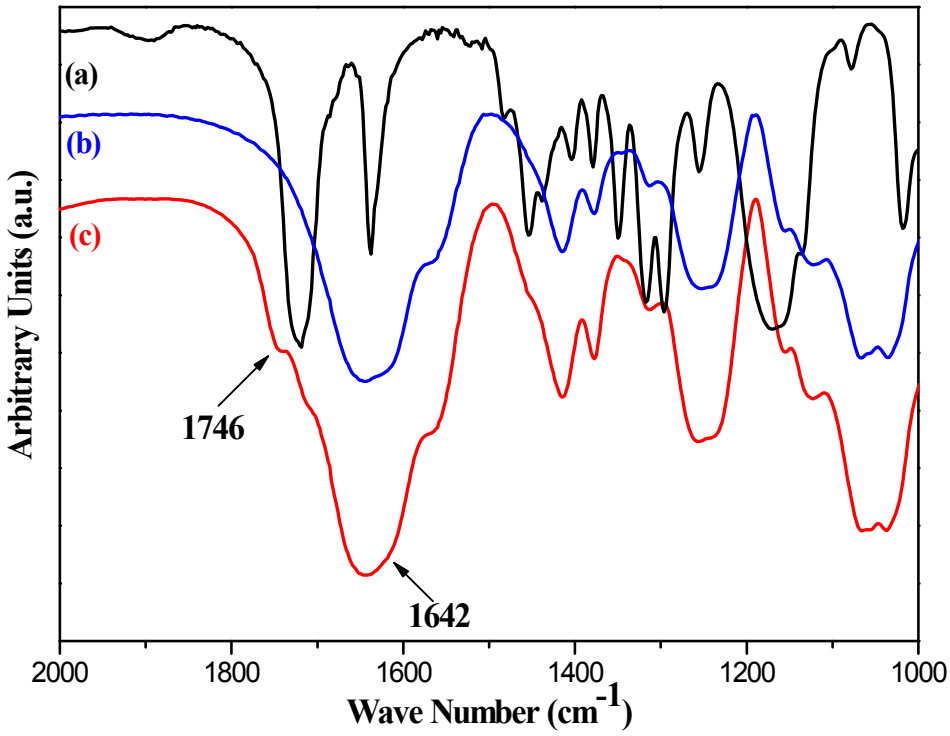

Figure S2. FTIR spectra of GMA (a), CS (b) and CS-methacrylate (c).

In the Figure S3 is shown the ^{1}H NMR spectra of the pristine CS, GMA and CS-methacrylate. The signals at δ 6.17 ppm and δ 5.77 ppm for the spectrum of CS-methacrylate are assigned to vinyl carbon-linked hydrogen (hydrogen 8 and 8'- numbered in the structure). The appearance of a signal at δ 1.95 ppm in the spectrum of CS-methacrylate is attributed to hydrogen of methyl groups at the vinyl carbons (labeled as 9 in the structure). The presence of signals 8, 8'and 9 indicates the modification of chondroitin sulfate with GMA [4].

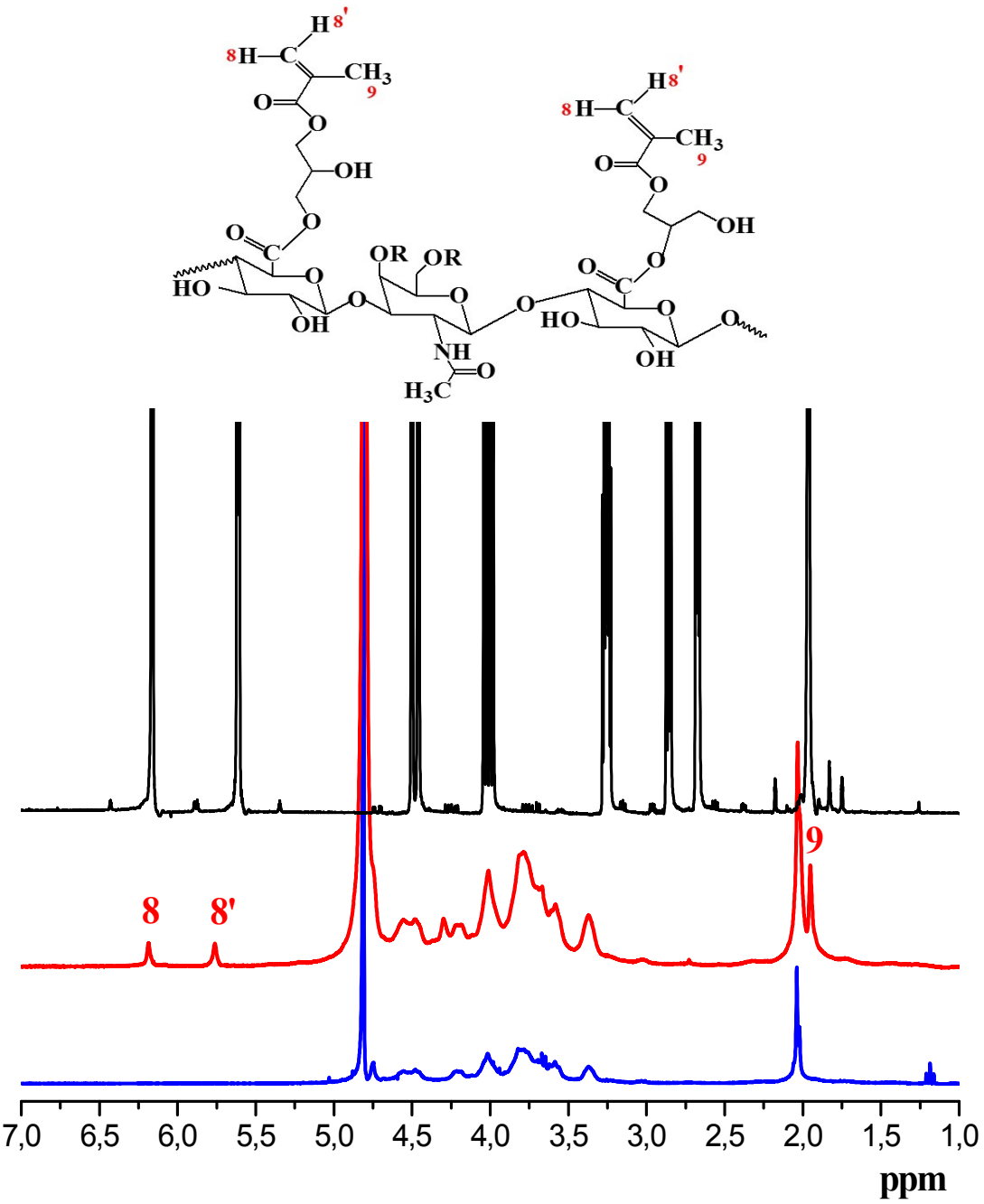

Figure S3. ^{1}H NMR spectrum of pristine CS (blue), CS-methacrylate (red), GMA (black) and the structure of CS-methacrylate.

The characterization of the chemical modification of CS with GMA was also done using ^{13}C NMR. In the Figure S4 ^{13}C-CP/MAS NMR spectra of pristine CS and CS-methacrylate are

presented. Some changes are verified in the spectrum of CS-methacrylate in relation to the CS in the region between 141 and 120 ppm. The signals present in this region corresponding to vinyl groups (unsaturated carbons) in the structure of CS-methacrylate (C1 and C2 as presented in the structure scheme in Figure 8). The peak at 165 ppm was assigned to carbonyl carbon of conjugated systems (C4) and the signal of the peak at 15.3 ppm relating to the methyl carbon derived from the structure of GMA (C3).[1, 4]

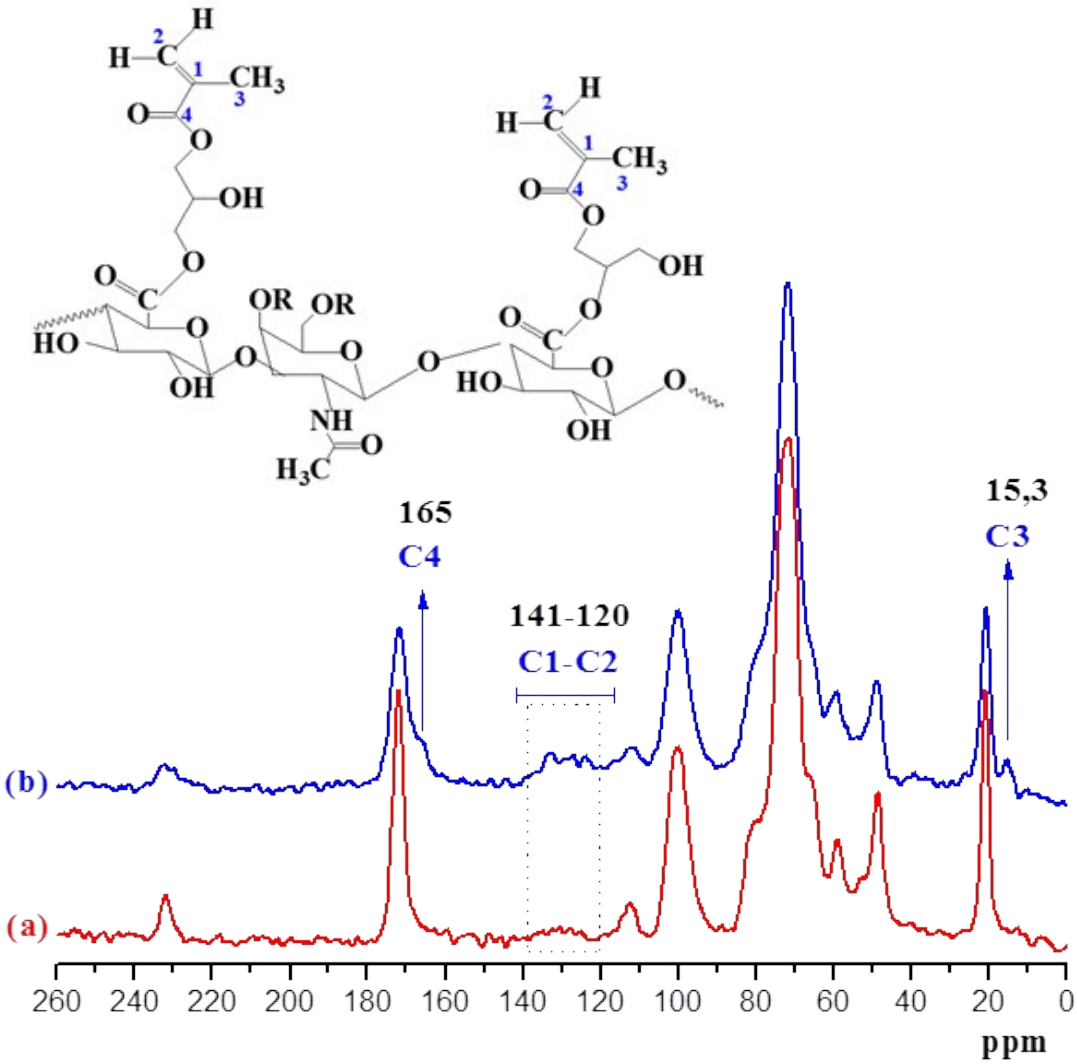

Figure S4. ^{13}C-CP/MAS NMR spectra of CS (a) and CS-methacrylate (b).

In the Figure S5 is shown the SEM images of CS and CS-methacrylate. In the SEM image of CS it is verified that CS has no regular arrangement of the polymer in the solid state. However, SEM images of CS-methacrylate, Figure S5 (b), evidenced polymer morphology quite different than observed for pristine CS, in which the modified polymer in the solid state tends to form more defined spherical particles. The tendency of forming particles instead of blocks as observed in the SEM images demonstrates that chemical modification of the CS also provides changes in the physical properties of polysaccharide, such as the intermolecular interaction.

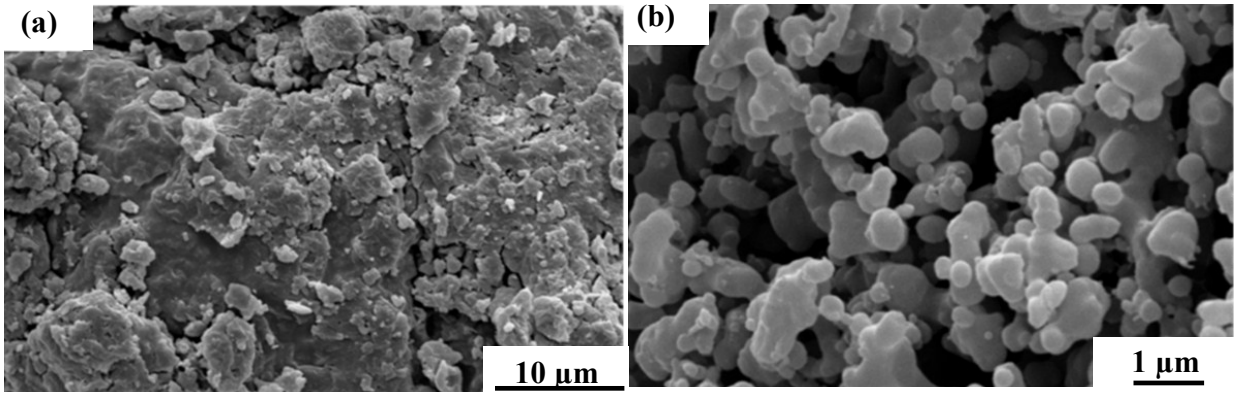

Figure S5. SEM images of CS (a) and CS-methacrylate (b)**.**

3. FTIR spectra of -HA-CS microspheres

The characterization of the crosslinking reaction and the formation of microspheres by FTIR were not as efficient, since the bands of interest, the double bond, fall on a characteristic region of chondroitin sulfate, in 1640 cm^{-1}, and thus can be observed only a small decrease in the intensity of this band, as shown in Figure S6. However it was possible to observe the appearance of the bands relating n-HA in the region of 1040, 602 and 566 cm^{-1} characteristic of stretch the P-O bond present in the n-HA. These data show that the emulsification method is suitable as a means for incorporating n-HA.

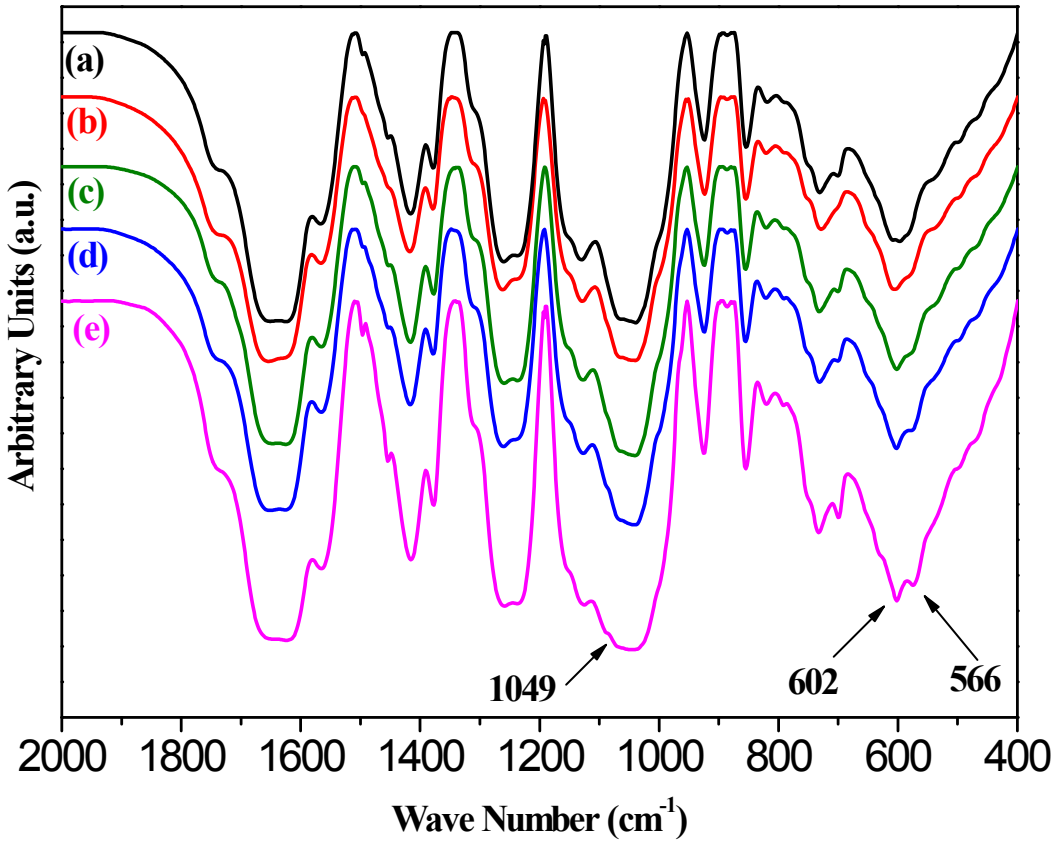

Figure S6. FTIR spectra for the n-HA-CS microspheres containing 1% n-HA (a), 3% n-HA (b) 5% n-HA (c) 7% n-HA (d) and 10% n-HA (e).

X-ray diffraction patterns of CS microspheres and n-HA-CS

In the Figure S7 are shown the WAXD patterns of CS microspheres and n-HA-CS microspheres containing 1%, 3%, 5%, 7% and 10% of n-HA. By Wide-angle X-ray diffraction patterns was possible to observe the major peaks characteristic of n-HA at 2θ equal to 25,6º, 31,8º and 32,9º concerning the planes (002), (211) and (300) respectively.

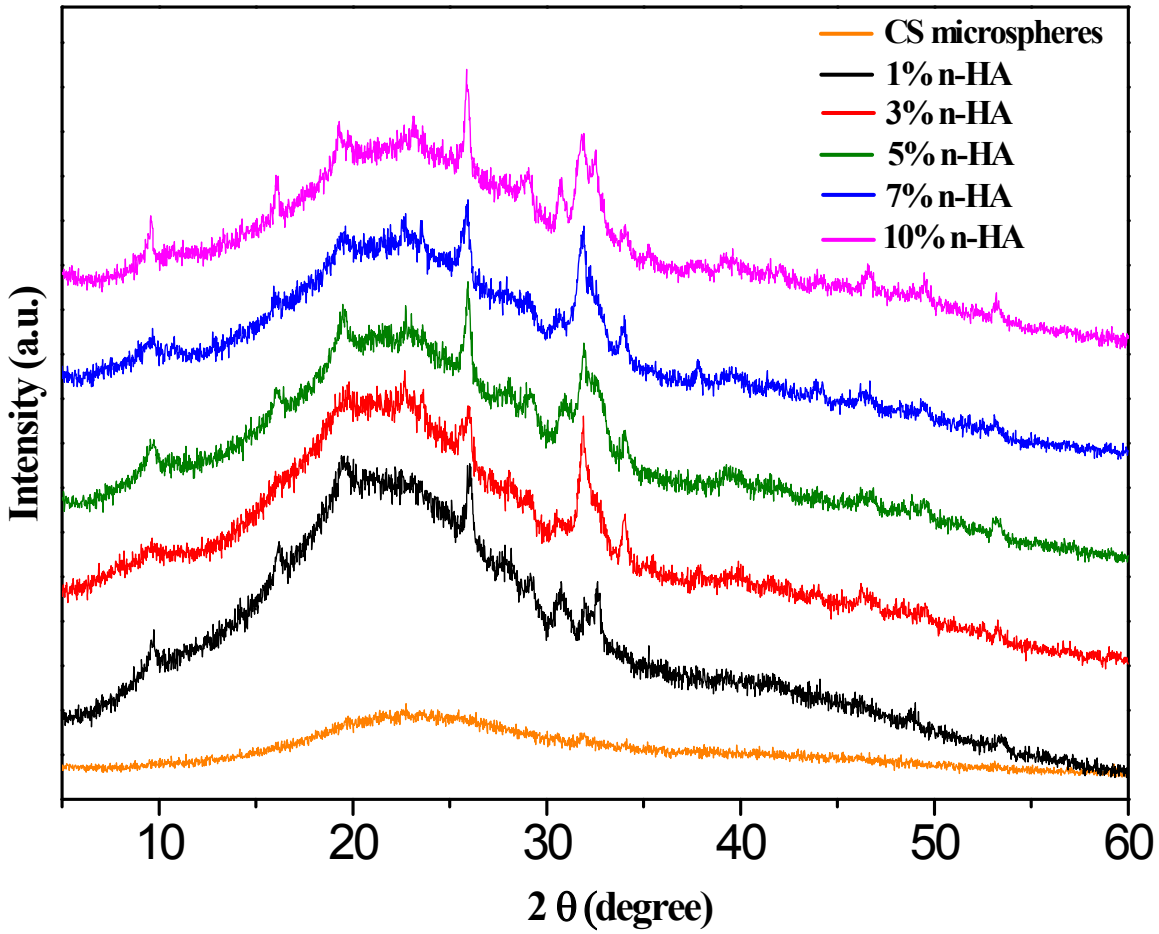

Figure S7. X-ray diffraction patterns of CS microspheres and n-HA-CS microspheres containing 1% , 3% , 5% , 7% and 10% n-HA.

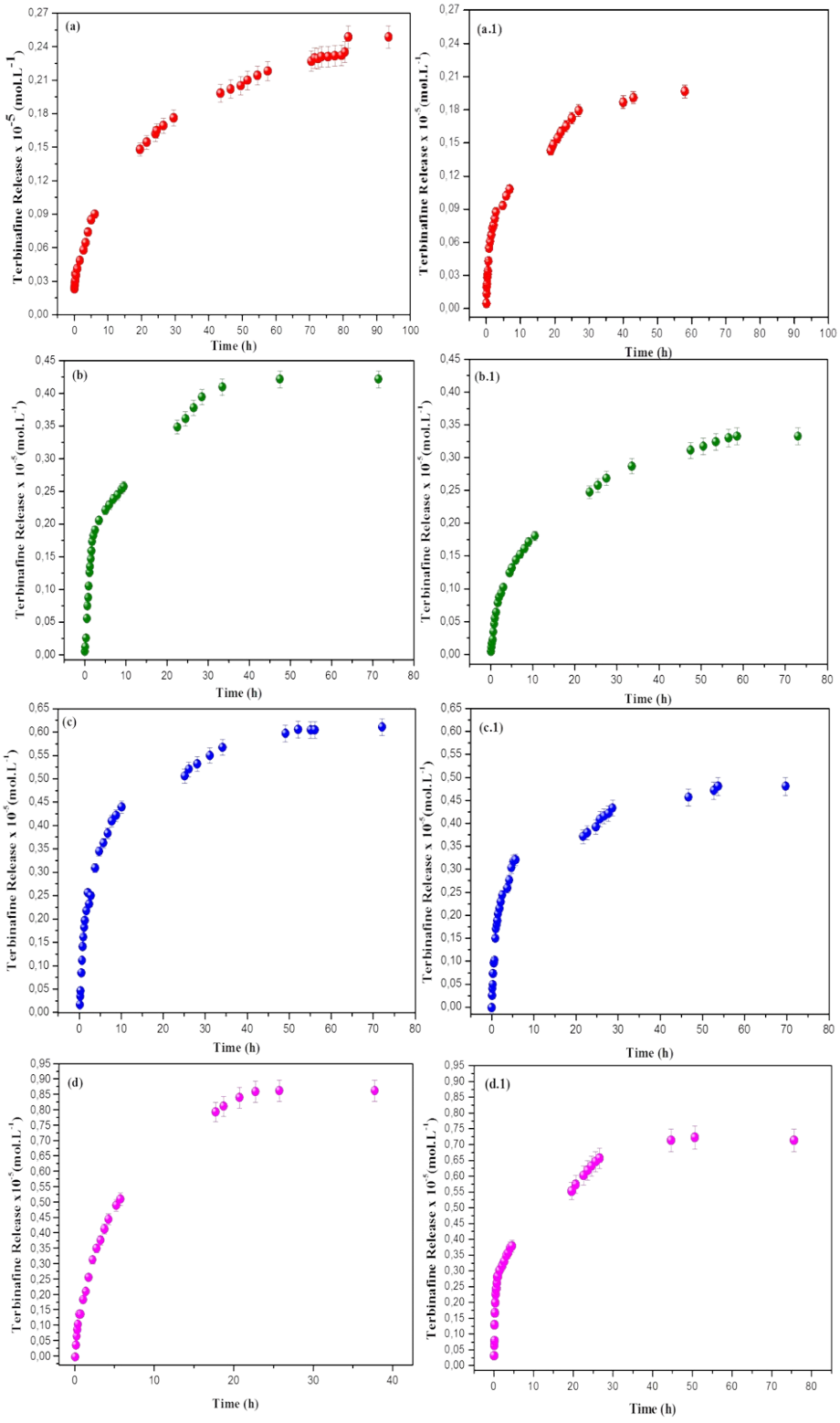

Fig. S8. Time-dependent release curves of Terbinafine in SGF from microspheres containing 3% (a), 5% (b), 7% (c) and 10% (d) of n-HA and in SIF from microspheres containing 3% (a.1), 5% (b.1), 7% (c.1) and 10% (d.1) of n-HA.

Fitting of Release Profiles

The release profiles of TB, correlating the released concentration in function of time, were fitted using equation 1 known as Korsmeyer-Peppas model for the CS microspheres containing different content of HA.[5-7] Korsmeyer-Peppas model is a broad used model for the study of releasing mechanism from polymeric systems.[5-7]

$$Wt/Weq = kt^n \qquad \textbf{(Equation 1)}$$

W_t and Weq are the weight of drug released at a specific time and the weight of drug released at the equilibrium point, respectively. k is a proportionality constant that is influenced by geometric and structural features of the drug delivery system, and n is the diffusion coefficient.

Equation 1 can be applied to the analysis of different drug delivery systems with different morphologies, including films, cylinders disks, and spheres. In addition, the fitting is done for the release intervals from zero to 60% of released drug. A linear equation (Equation 2) can be obtained by applying the logarithmic form of the equation 1.

$$\log \frac{Wt}{Weq} = n\, logt + logk \qquad \textbf{(Equation 2)}$$

A straight line should be obtained in a graphic of *log* of the drug's released fraction in function of time, where the angular coefficient corresponds to n. It was found that the value of n can be correlates with the geometry of the drug delivery system and the releasing mechanism,[6] as presented in Table S1.

Table S1. Diffusion coefficient by Korsmeyer-Peppas model and releasing mechanism to different geometric systems.[6]

Diffusion Coefficient, ***n***			
Thin Films	**Cylinders**	**Spheres**	Releasing Mechanism
0.5	0.45	0.43	Fickian Diffusion
$0.5<n<1.0$	$0.45<n<0.89$	$0.43<n<0.85$	Anomalous Transport
1.0	0.89	0.85	Case-II Transport
>1.0	>0.89	>0.85	Super caso-II Transport

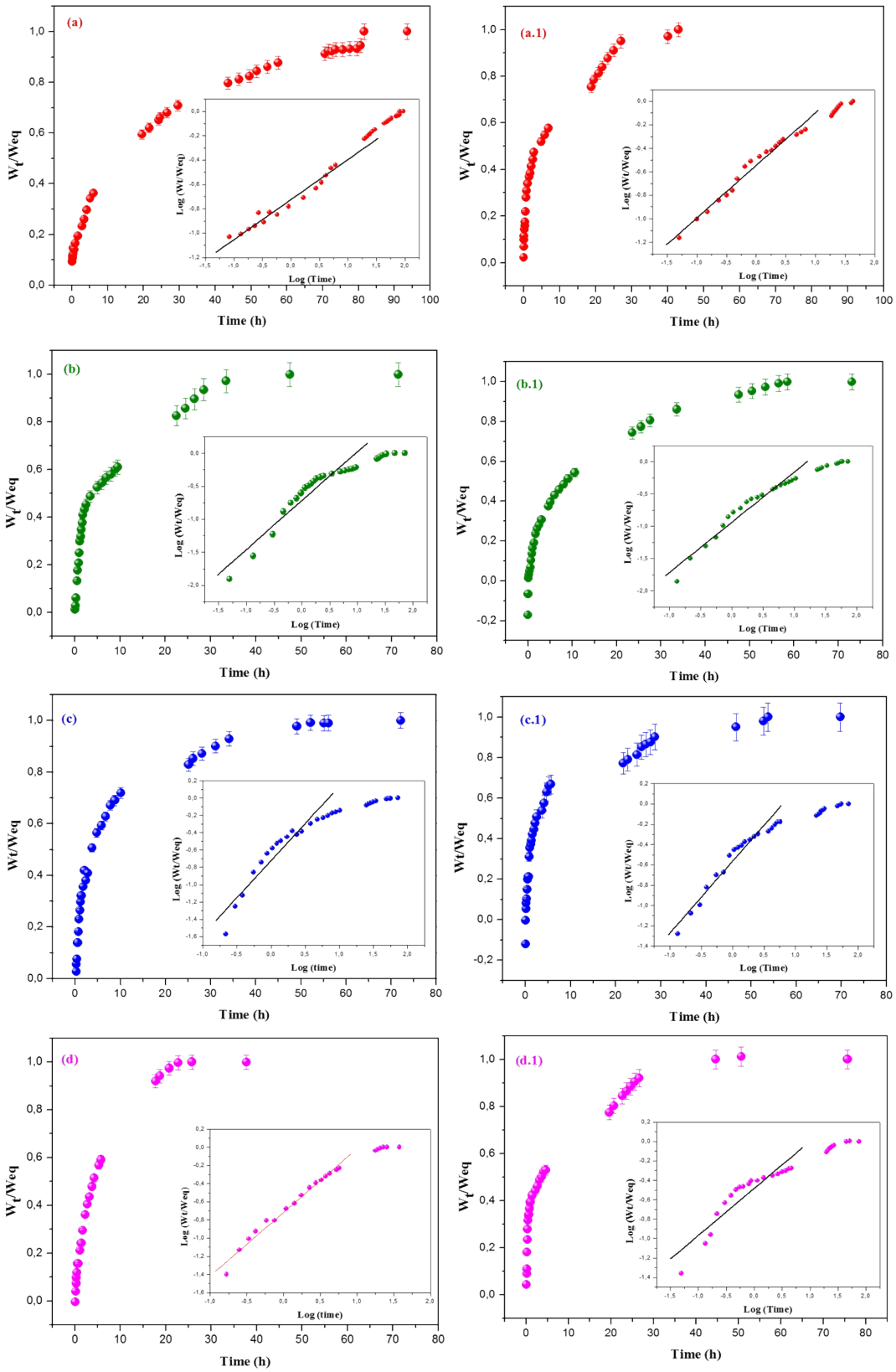

Fig. S9. Time-dependent release curves of Terbinafine and inserts with *log* of the drug's released fraction in function of time in SGF from microspheres containing 3% (a), 5% (b), 7% (c) and

10% (d) of n-HA and in SIF from microspheres containing 3% (a.1), 5% (b.1), 7% (c.1) and 10% (d.1) of n-HA.

The releasing mechanism by Fickian diffusion is the mechanism in which the drugs diffusion through the drug delivery system matrix is exclusively determined by Fickian diffusion. Case-II transport is controlled by the swelling and relaxation of the drug delivery system matrix and it is independent of time. In the case of anomalous transport, the drug delivery is due the both Fickian diffusion and swelling and relaxation of the drug delivery system matrix. In the super case-II transport, the release is ruled by the macromolecular relaxation of the polymeric chains.[7] In Figure S9 are presented the release profile of TB from CS microspheres containing different content of HA in both SGF and SIF. In the Table S2 and S3, are presented the values of *n* for the different simulated fluids and also the classification according to the releasing mechanism.

Table S2. Diffusion coefficient (*n*) and classification of release mechanism for the microspheres containing HA and TB simulated gastric fluid (SGF).

HA content	**Diffusion coefficient (*n*)**	**Mechanism**
3 %	0.33	Not attributed
5 %	0.73	Anomalous Transport
7 %	0.85	Case-II Transport
10 %	0.69	Anomalous Transport

Table S3. Diffusion coefficient (*n*) and classification of release mechanism for the microspheres containing HA and TB simulated intestinal fluid (SIF).

HA content	Diffusion coefficient (*n*)	**Mechanism**
3 %	0.44	Fickan Diffusion
5 %	0.77	Anomalous Transport
7 %	0.70	Anomalous Transport
10 %	0.48	Anomalous Transport

References

1. A. V. Reis, A. R. Fajardo, I. T. A. Schuquel, M. R. Guilherme, G. J. Vidotti, A. F. Rubira and E. C. Muniz, *Journal of Organic Chemistry*, 2009, **74**, 3750-3757.
2. A. V. Reis, M. R. Guilherme, L. H. C. Mattoso, A. F. Rubira, E. B. Tambourgi and E. C. Muniz, *Pharmaceutical Research*, 2009, **26**, 438-444.
3. R. Silva, E. C. Muniz and A. F. Rubira, *Langmuir*, 2009, **25**, 873-880.

4. M. R. Guilherme, A. V. Reis, B. R. V. Alves, M. H. Kunita, A. F. Rubira and E. B. Tambourgi, *Journal of Colloid and Interface Science*, 2010, **352**, 107-113.
5. Ritger P. L., Peppas N. A., *Journal of Controlled Release*, **1987,** 5, 23.
6. Ritger P. L., Peppas N. A., *Journal of Controlled Release,* **1987**, 5, 37.
7. Korsmeyer R. W, Gurny R., Doelker E., Buri P., Peppas N. A., **1983**, 15, 25.